www.czasopisma.pan.pl PAN POLSKA AKADEMIA NAUK www.journals.pan.pl

Arch. Metall. Mater. **67** (2022), 2, 521-527

DOI: https://doi.org/10.24425/amm.2022.137785

M.C. PERJU[1,2,3], C. NEJNERU[1], P. VIZUREANU[1,2,3], A.A. AELENEI[1], A.V. SANDU[1,2,3*], L. SACHELARIE[4], M. NABIAŁEK[5]

SOME ASPECTS CONCERNING TITANIUM COVERAGE WITH HYDROXYAPATITE

Generally, the metallic implants do not exhibit any bio-integration properties in contact with bone tissues. To improve the interfacial properties of metallic implants in contact with bone, the coatings with thin biocompatible films are used. Two methods to coating titanium implants with hydroxyapatite are described. The first is a two phase method, where by cathodic polarization is deposed a monetite film followed by an alkaline treatment when the monetite is converted to hydroxyapatite. The second method is a biomimetic deposition on an alkaline activate titanium surface, using a five time more concentrated simulated body fluid (5xSBF). After deposition this samples was drying at 120°C and was sintered at 700°C for three hours. Optical microscopy, Fourier Transform Infrared Spectroscopy (FTIR), Scanning Electron Microscopy (SEM) and Energy-dispersive X-ray (EDX) were used to characterize structure, morphology and compositions of the deposed films. In this study, electrochemical deposition and biomimetic deposition of hydroxyapatite are compared.

Keyword: Hydroxyapatite; Monetite; Electrochemical and Biomimetic Deposition; FTIR; SEM

1. Introduction

In practice of the metallic implant utilization a modification of the implant surface is evermore necessary [1-3]. These transformations search the surface improvement to increase their biocompatibility and ossteointegration [4,5].

Chemical etching of surface improve the physical adherence, the oxidation (in the titanium case) assure a protection to externally influence and a best tolerance of human tissue [6]. The chemical activation brings the ionic groups on surface and favors the cell-implant interaction. However, the best procedure rest in the surface coating with biocompatible materials, such as ZrO_2, calcium phosphates and mainly hydroxyapatite $(Ca_{10}(PO_4)_6(OH)_2$.

The coating procedure is nevertheless limited to very small implants, without being subjected to high loads, due to of their mechanical properties, especially fracture toughness and elasticity modulus and due to their poor adhesion to the metallic substrates.

Plasma or thermal spraying of hydroxyapatite (HA) has been widely used for this purpose and has received commercial success over other alternatives [7,8]. However, plasma spraying operates under extremely high temperatures, e.g. 6000-10.0001°C, and thus can easily destabilize the crystal structure of HA, causing its decomposition into a mixture of HA, CaO, tricalcium phosphate, tetra calcium phosphate and considerable amount of amorphous phases. Severe cracking of the coating layer is frequently observed, primarily due to rapid temperature fluctuations and solidification of the coating.

More methods for HA coatings of implants include: electrophoretic deposition [9], electrochemical deposition [10,11], laser-pulse deposition [12], ion-beam deposition [13], and sol–gel deposition [14]. Other interesting alternatives of obtaining these biocompatible coatings are electrodeposition [15,16], electrophoresis [17] and biomimetic deposition [18,19]. These processes are developed at room temperature and have many advantages over other, more commercial deposition processes, such as: uniformity of the deposited layer, availability of various substrate shapes other than plates, good control of the deposition thickness and quality, low energy consumption and also the fact that it is an environmentally friendly process.

[1] "GHEORGHE ASACHI" TECHNICAL UNIVERSITY OF IASI, FACULTY OF MATERIALS SCIENCE AND ENGINEERING, PROF. D. MANGERON STREET, NO. 41, 700050, IASI, ROMANIA
[2] UNIVERSITI MALAYSIA PERLIS (UNIMAP), CENTRE OF EXCELLENCE GEOPOLYMER AND GREEN TECHNOLOGY (CEGEOGTECH), PERLIS, MALAYSIA
[3] ROMANIAN INVENTORS FORUM, SF. P. MOVILA 3, IASI, ROMANIA
[4] APOLLONIA UNIVERSITY OF IASI, FACULTY OF DENTISTRY, PACURARI STREET, NO. 11, 700511, IASI, ROMANIA
[5] CZĘSTOCHOWA UNIVERSITY OF TECHNOLOGY, DEPARTMENT OF PHYSICS, 42-200 CZĘSTOCHOWA, POLAND

* Corresponding author: sav@tuiasi.ro

Also, in dental and orthophaedic applications titanium implants with porous surfaces or with superficial nanotube structure were used. Porous surface structure improves osseous-integration because it provides spaces for anchoring bone cells and for vascular and bone tissue ingrowths.

In this study, electrochemical deposition and biomimetic deposition of hydroxyapatite are compared. The electrochemical method was presented in the paper [20], evidencing, by X-ray diffraction, that the hydroxyapatite formation take place in two steps, via monetite. Also, in a review paper [21], Sylwia Sobieszczyk describes the electrochemical and biomimetic methods for hydroxyapatite coatings onto nanotubular titanium oxide layers formed on Ti and Ti alloys.

For the electrochemical methods both one step and two steps are described. In the case of biomimetic method the nanotubes structure of metal surface assure a best deposition of hydroxyapatite, due to the fact that nanotubes offer a large specific surface area.

The electrochemical deposition is a relative fast method which is useful in the case of implants with complicated shape and surface, while the biomimetic method is rather a natural deposition of the hydroxyapatite on an implant introduced in human body, there in vitro simulation being helpful for the knowledge of the natural deposition processes.

In this study we achieve an additional approach of the electrochemical and biomimetic hydroxyapatite deposition in the initial steps of the processes.

2. Materials and methods

2.1. Materials

Pure titanium plates were used as substrate for hydroxyapatite coating. The titanium plates (12×12×5 mm) were firstly cleaned ultrasonically, successively, with acetone, ethanol and water for 10 minutes each before being to be used. For better electrochemical and biomimetic deposition the surface was roughened by acid etching, and activated. The surface etching was made immersing the sample into a solution of 48% H_2SO_4 + 18% HCl, at 60°C, for 90 minutes.

2.2. Electrochemical coating

For the electrochemical deposition of hydroxyapatite we choose the two-step method, through the monetite formation in the first step and monetite-hydroxyapatite conversion in the second step. For this purpose o potential difference of 2000 mV between titanium (cathode) and platinum (anode) was applied for 25 minutes.

The electrolyte medium was a solution rich in Ca^{2+} and PO_4^{3-} ions, hawing the composition: 0.5M $Ca(OH)_2$, 0.5M H_3PO_4 and 1M CH_3CHCO_2HOH (Lactic acid). The electrochemical reaction was conducted in an electrochemical cell with three electrodes, the reference being a saturated calomel electrode. The cathodic deposition was carried out with a VOLTALAB 21 potentiostat/galvanostat (PGZP 201 type – Radiometer Copenhagen), in chrono-amperometry regime. The temperature was maintained around 75°C. During the deposition process the current density have been varied between 0.6 and 0.2 mA/cm^2. The variation of current density during deposition is presented in Fig. 1.

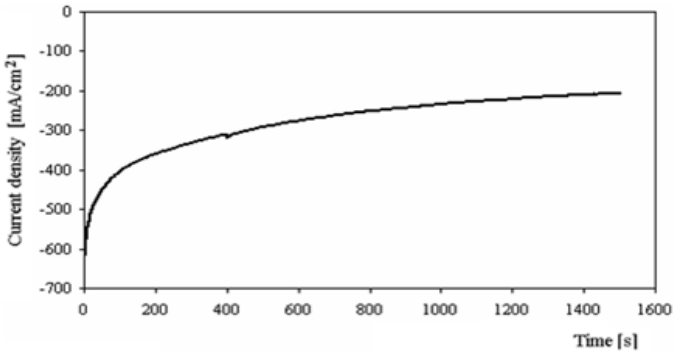

Fig. 1. Current density variation during electrochemical deposition

The treated sample was washed with deionised water and dried at 120°C. In the second step the sample was immersed 0.1 M NaOH for 67 hours at ambient temperature and after drying at 55°C was sintered at 700°C for three hours.

2.3. Biomimetic deposition

This process is based on heterogeneous nucleation of calcium phosphate from Simulated Bode Fluid (SBF) at pH = 7.4 and a temperature of 37°C. The deposition takes place after an immersion of 14-28 days of metal in solution.

For a good deposition and for reducing the deposition time, metallic sample need roughened and activated. The etching was performed in mixed acid (34% H_2SO_4 + 12% HCl), at 65°C for 90 minutes. The activation was made electrochemically in Habibovic solution (40 g NaCl; 1.39 g $CaCl_2$; 1.52 g $MgCl_2$; 1.06 g $NaHCO_3$; 0.89 g $Na_2HPO_4 \times 12H_{20}$; 40 ml HCl 1M / per liter) [22,23]. This solution was buffered and stabilized with trietanol amine (1/4) and acidified with HCl to pH = 6.4. In activation cell, the sample was polarized to anode for 10 minute at a potential of 2 V.

This electrochemical activation assures to forms the crystallization centers on titanium surface.

The microstructure of etched surface and the time variation of current density during the activation process are presented in Fig. 2.

After activation the sample was intensively washed with distilled water in an ultrasonic cleaner, and immersed into a saturated Ca-P solution for 68 hours at ambient temperature. The concentrations of calcium and phosphorus solution were 5 times concentrated than those in human body fluid.

The composition of the concentrated Simulated Body Fluid (5xSBF) vas: 43 g NaCl; 1.5 g $MgCl_2 \times 6H_2O$; 1.4 g $CaCl_2 \times 2H_2O$;

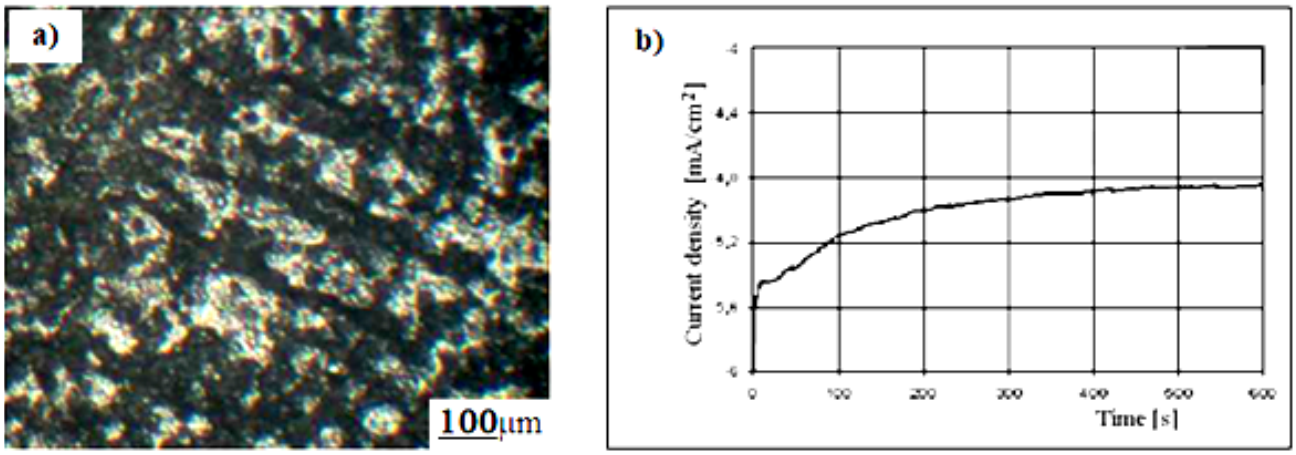

Fig. 2. Surface micrography of chemical etched titanium (a) and chrono-amperometric curve (b)

1.7 g Na_2HPO_4; and 1.63 g $NaHCO_3$ per liter. After deposition this samples was washed with distilled water and dried in air at 120°C. Finally, the sample was calcined in air for three hours at 700°C.

3. Results and discussion

3.1. Characterization of Optical microscopy

The surface features after the electrochemical and biomimetic treatment was firstly examinated with an optical microscope OLYMPUS PME-3 ADL (Frank Bacon Machinery Sales Co) and is presented in the Fig. 3.

Taking into account the very short times of depositions, 25 minutes in the electrochemical method and 68 hours in the biomimetic method, these depositions can be considered only as primarily processes. The images from Fig. 3 marking out the fact that the electrochemical method is faster and assure a good deposition, while in the biomimetic method arise only a nucleation of hydroxyapatite phase.

3.2. Characterization of Fourier Transform Infrared Spectra (FTIR)

Since the deposed hydroxyapatite quantity in the two methods are very little, especially in biomimetic deposition, for Fourier Transform Infrared Spectra (FTIR) acquisition was used a micro-Spectrophotometer TENSOR 27 coupled with an Hyperion 1000 microscope (Bruker Optics, Germany), controlled with the OPUS software. The registered spectrum after the electrochemical treatment is presented in Fig. 4.

The peaks at 1150, 1052, 960 shoulder, 563 and 598 were attributed to the characteristic vibrations of PO_4^{3-} (the 1150, 1052 and 960 peaks arise from stretching vibrations of P-O bonds, the 563 and 598 can be due to bending mode in O-P-O(H) groups) [24]. This spectrum corresponds to the $CaHPO_4$, and confirms that the deposed material in the first step is $CaHPO_4$ – Monetite.

The conversion of monetite to hydroxyapatite, $CaHPO_4 \rightarrow (Ca_{10}(PO_4)_6(OH)_2)$, was realized immersing the covered sample in 0.1M NaOH for 67 hours at ambient temperature. After intense washing and drying to 55°C for three hours, the micro-FTIR spectrum was registered. This spectrum is illustrated in Fig. 5.

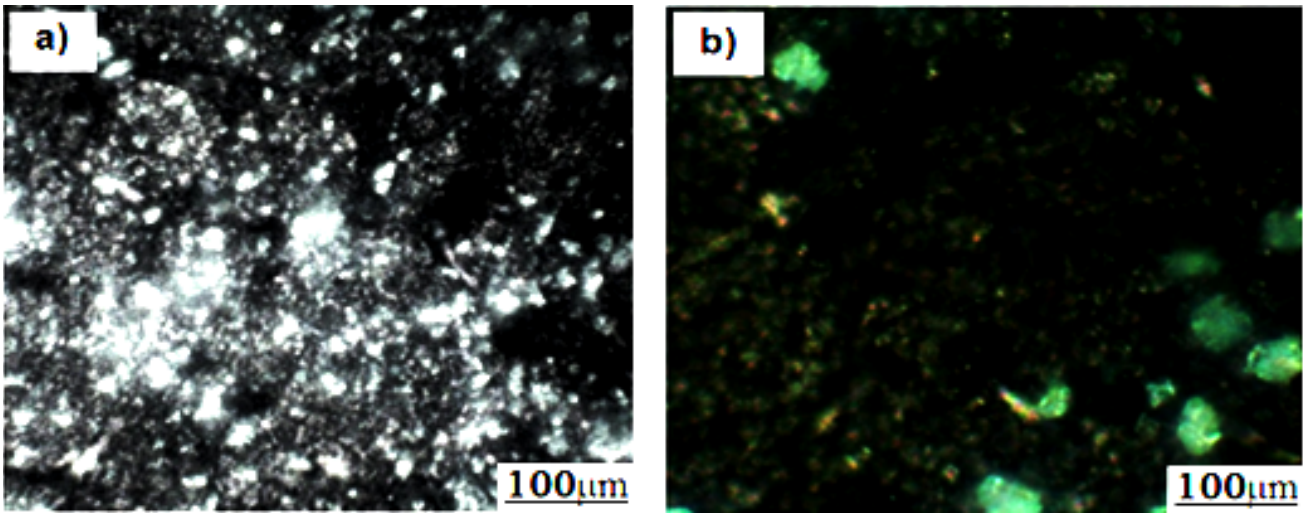

Fig. 3. Optical microscopy after hydroxyapatite deposition: electrochemical method (a) biomimetic method (b)

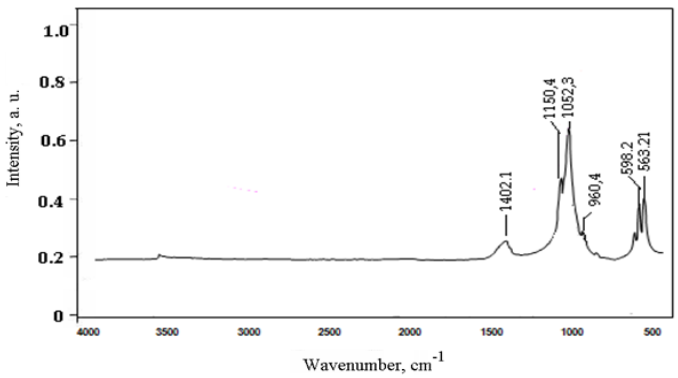

Fig. 4. Micro-FTIR spectrum of the deposed material after electrochemical treatment

The band registered at 973 cm^{-1} is attributed to bending vibration of P-O bond, while the strong bands 1012 and 1100 cm^{-1} evidence the P-O stretching vibrations in PO_4^{3-} group [25]. The peak 3557 cm^{-1} is attributed to the stretching vibration of HO^- group in the hydroxyapatite lattice while the very broad band's at 3483 and 3098 are related to free absorbed water in hydroxyapatite layer. Also, the strong peak at 1653 cm^{-1} is associated also with absorbed water. The broad and intense bands in the high wave number domain indicate a deficient drying of the simple. The main hydroxyapatite absorption bands there are recognized in this spectrum but they are a little displaced under the influence of the adsorbed water.

The registered spectrum after burning of the converted sample is illustrated in Fig. 6. In the domain of high wave number were remained only a little two bands, associated to symmetric stretching O-H bond in structural OH (3571 cm^{-1}) and free H_2O (3544 cm^{-1} shoulder). The little peak at 638 cm^{-1} is attributed also to vibrational mode of structural O-H bond.

The bands associated with characteristic vibrations in PO_4^{3-} are clearly definite: 960 cm^{-1} symetric stretching vibrations of P-O, strong bands found at 1081 and 1124 cm^{-1} associated to vibration mode of the functional group PO_4^{3-}. The bands at 881, 14011 and 1460 cm^{-1} are peaks characteristic for CO_3^{2-} carbonate. The presence of the carbonate ions in hydroxyapatite struc-

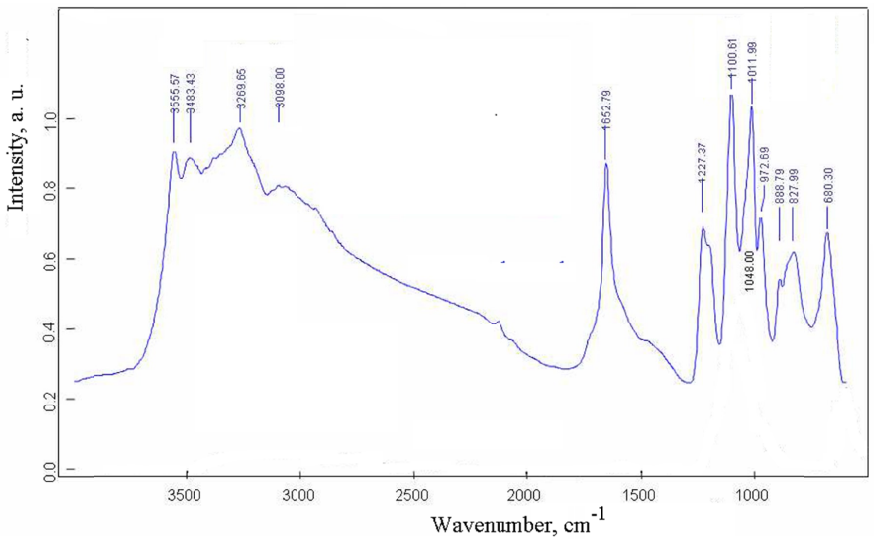

Fig. 5. Micro-FTIR spectrum for sample after conversion monetite/hydroxyapatite treatment

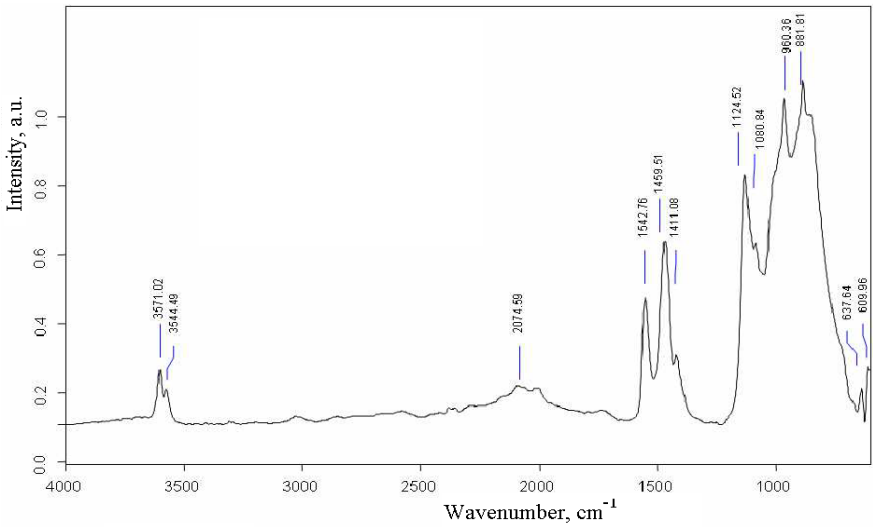

Fig. 6. Micro-FTIR spectrum for electrochemical deposition after monetite/hydroxyapatite conversion and calcination at 700°C for 3 hours

ture is due to the fact that in the during of the calcination process atmospheric CO_2 reacts with structural or absorbed OH^- forming carbonate ions [26]. The characteristic bands in this spectrum are narrow and wery well definite, indicating a cristalisated carbonated hydroxyapatite.

In the case of the biomimetic deposition the micro-FTIR spectrum vas obtained only for the one deposed nucleus, and is presented in Fig. 7 by comparation with hydroxyapatite spectrum.

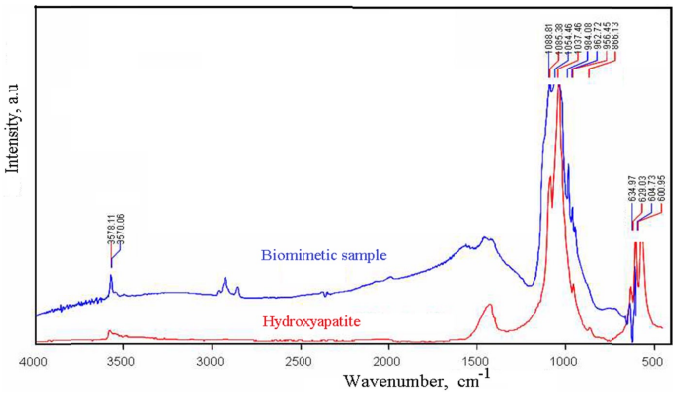

Fig. 7. Micro-FTIR spectrum for the biomimetic deposed sample

One can see a very good agreement between the two spectra, this denoting that, really, by this method the pure hydroxyapatite was formed. The main disadvantage of biomimetic method is the very long time for a consistent layer formation.

3.3. Characterization of Scanning Electron Microscopy (SEM) and Energy-dispersive X-ray (EDX)

The structure and superficial composition of the deposed material in the three stage of the electrochemical method are characterized by Scanning Electron Microscopy (VEGA II LSH – Tescan Co., Czechoslovakia) and with Energy Dispersive X-ray Analysis, using a micro-detector EDX QUANTAX QX2 (Bruker/Roentec Co., Germany). Fig. 8 illustrate to evolution of the deposed layer after the coating steps.

From the figures, one can see that the morphology of deposed layer changes from a microcristaline monetite, to a noncrystalized agglomerations of hydroxyapatite with irregular granular shape and, finally, to a sintered material with well formed crystals. The EDX microanalysis, presented succinctly in Fig. 9, confirm the initial assumption and SEM evidences.

The atomic ratios between the main components of the deposed material, Ca and P, allow identifying the basic compound of the layer. Thus, in the layer deposed electrochemically, the atomic ratio n(Ca)/n(P) = 0.929, very closed to 1.00, characteristic for pure monetite ($CaHPO_4$). After alcaline conversion the atomic ratio n(Ca)/n(P) = 1.455 correspond to a calcium deficient hydroxyapatite ($Ca_9(HPO_4)(PO_4)_5OH$), of that this ratio is 1.50. This fact denotes that the conversion monetite/hydroxyapatite was only partially realized.

For calcinated sample n(Ca)/n(P) = 1.626, closed to ideal value of 1.667 characteristic for pure hydroxyapatite. This little

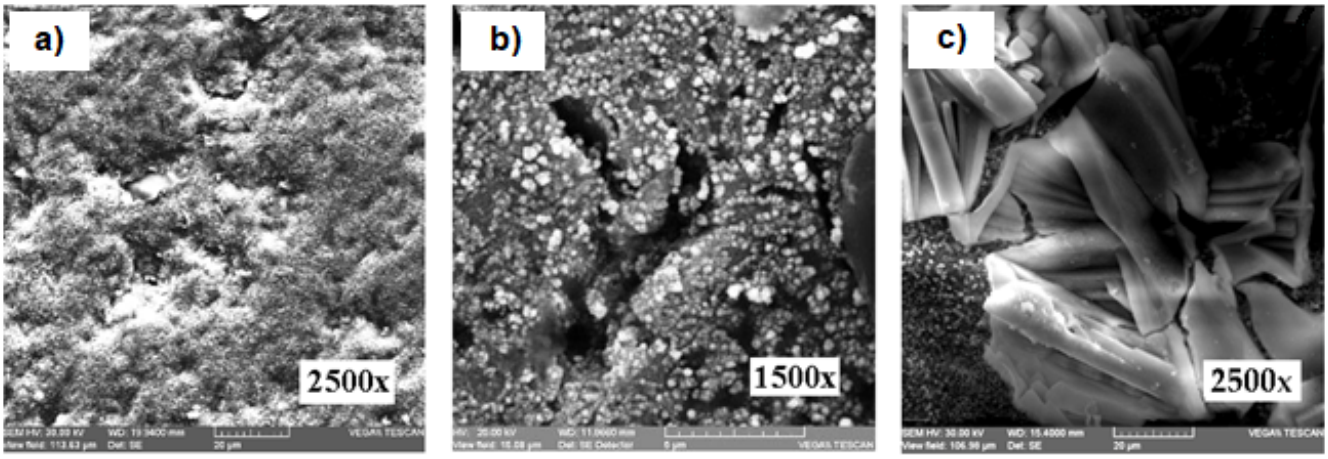

Fig. 8. SEM micrographs of the coated material on titanium plate: after electrochemical deposition (a), after monetite/hydroxyapatite conversion (b) and after calcination at 700°C for 3 hours (c)

After electrochemical deposition			After monetite/HA conversion			After calcination		
Element	norm. at.-%]	Error in %	Element	m. at.-%]	Error in %	Element	norm. at.-%]	Error in %
Calcium	13,11433	0,720746971	Calcium	22,2583	1,237926	Calcium	25,134116	1,30510002
Phosphorus	14,1230371	0,834262878	Phosphorus	15,0246	0,879483	Phosphorus	15,458469	0,82340551
Titanium	2,13675419	0,164666548	Titanium	1,09369	0,153386	Titanium	0,382156	0,05378415
Oxygen	70,6248814	20,47139868	Oxygen	59,1827	6,688184	Carbon	1,116.876	0.092884
						Oxygen	57,9177835	27,125655
	Ca/P ratio=0.929			Ca/P ratio=1.455			Ca/P ratio=1.626	

Fig. 9. Base compositions of the deposed layer during deposition steps

difference can be attributed to the presence of calcium carbonate in the sintered sample.

The sample deposed by biomimetical method was also analyzed by Scanning Electron Microscopy and EDX microanalysis. The SEM image of the surface and the EDX energetical spectra are presented in Fig. 10.

In zone A, which cover somewhere about the entire surface of the sample, one can see the surface rugosity of the base material obtained by etching and activation processes. The EDX energetical spectrum for this zone relieves only the presence of the titanium and titanium oxide. The EDX spectrum of a deposed hydroxyapatite nucleus, denoted as zone B, attest also that this nucleus is a calcium phosphate compound, most probable hydrtoxyapatite, beside titanium oxide and traces of absorbed ions from solution.

Fig. 11 shows the SEM image of the calcinated sample and composition of the deposed hydroxyapatite, evaluated by EDX.

From the figure one can see that the deposed HA nuclei were crystallized, but HA nucleus are partial detached from the sample surface.

This can be an indication that the adherence of the hydroxyapatite deposed biomimetically is rather weak.

The atomic ratio (nCa)/n(P) = 1.608 is just about to 1.667, the corresponding value for pure hydroxyapatite. Moreover, in the HA nucleus were identified adsorbed ions as Na^+ and Cl^-.

Our results are in a good agreement with those obtained by other authors. Thus, in the published results of Mareci et al., [20], the hydroxyapatite deposed on comercial pure titanium by electrochemical method was characterized by X-ray diffraction, Fourier Transform Infrared Spectroscopy and EDX microanalysis. As opposed to our study the cited authors do not report the deposition conditions. The XRD spectra confirm the three steps deposition of HA, via monetite. Further, by Electrochemical Impedance Spectroscopy measurements in Ringer solution, these

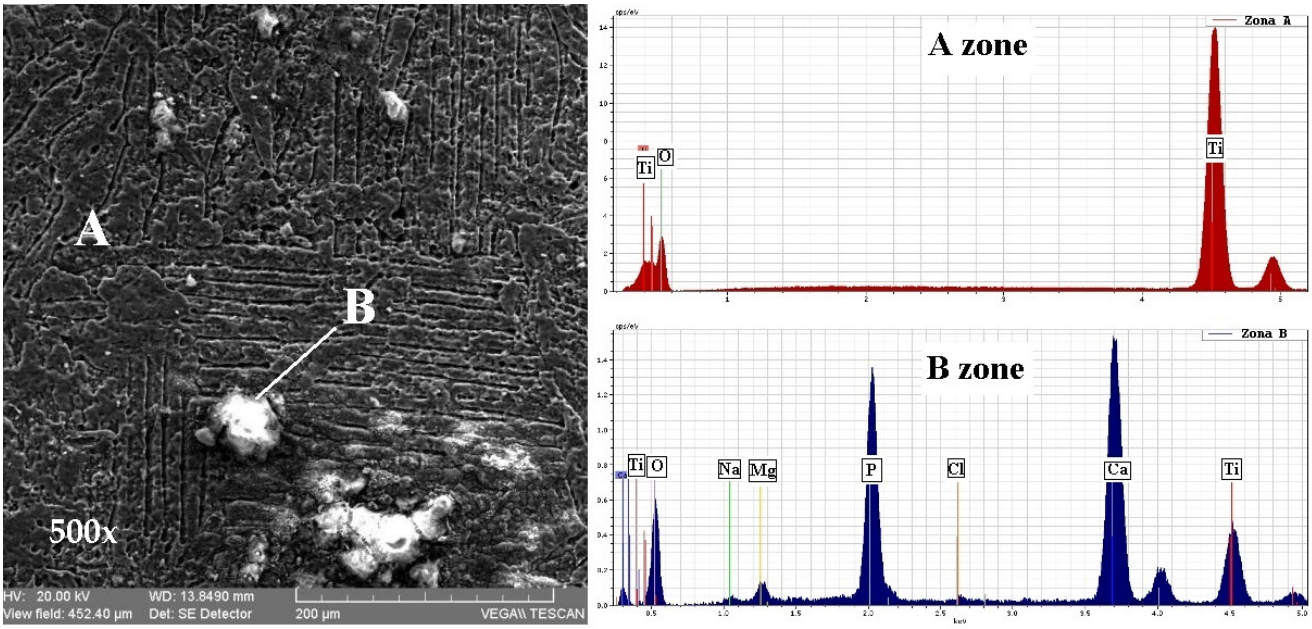

Fig. 10. EDX spectra for two zone of the sample treated surface: non covered zone (A); deposed nucleus (B)

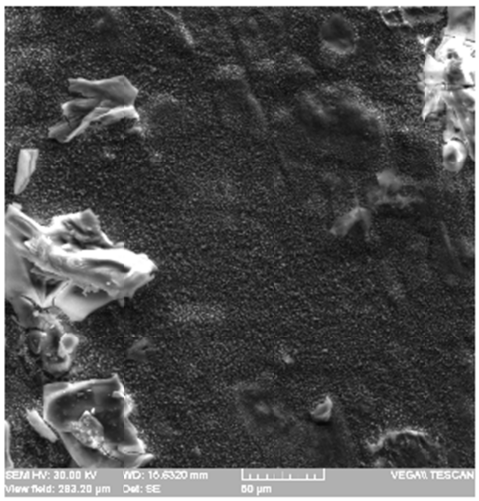

Element	Net	[wt.-%]	[norm. wt.-%]	[norm. at.-%]	Error in %
Calcium	120752	42,80705843	38,6447432	22,90254711	1,203540192
Phosphorus	69630	19,97238177	18,4616519	14,24213268	0,804171584
Sodium	1287	0,869087535	0,80334893	0,834964463	0,122218715
Titanium	1464	0,759093485	0,70167493	0,350171035	0,055752147
Chlorine	415	0,133310888	0,12322713	0,083053015	0,033855357
Oxygen	20766	44,4620494	41,0988979	61,37971643	27,51443104
	Sum:	108,1830699	100	100	
			n(Ca)/n(P) = 1.608		

Fig. 11. SEM micrograph of the sample treated biomimetically after calcination and EDX composition of the deposed hydroxyapatite

authors evidenced that the coated film appear as a double-layer model; a compact protective inner layer (most probable TiO_2) and a porous external layer (HA). The electrochemical and biomimetic depositions were reviewed by Sobieszczyk [21] analyzing the deposition of HA on porous titanium and titanium alloys. The presence of TiO_2 nanotubes enhances bond strenght improving the HA adherence to metallic substratum.

4. Conclusions

Among the metallic biomaterials used as orthopedic implants or dental implants, titanium and titanium alloys best meet the required conditions. They have a good biocompatibility due to a special resistance to corrosion in the human body, the formation of strong bonds between the implant surface and adjacent bone tissue and the values of modulus of elasticity that greatly reduce the adverse effects of bone remodeling. In the practice of using the metal implant, a modification of it is increasingly necessary. These transformations seek to improve the surface to increase their biocompatibility and osseointegration. Biocompatible thin film coatings are used to improve the interfacial properties of metal implants in contact with bone.

The coating of hydroxyapatite on titanium support was performed by electrochemical method, via monetite, in three steps: monetite deposition, alkaline conversion of monetite to hydroxyapatite and final calcinations to 700°C. The evolution of the covered surface was characterized by FTIR, SEM and EDX analysis, and confirms the initial suppositions and other results from literature.

The biomimetic deposition on titanium was realized using five times concentrated Simulated Body Fluid (5xSBF), and the results were characterized also with the same methods.

In both electrochemical and biomimetic coatings, the short times of deposition allowed to analyses the initial stages of the coatings. In the biomimetic method the initial stage suppose only the nucleation of the hydroxyapatite, and their adherence to titanium support is weak.

The biomimetic deposition method is performed in a much longer time interval than the electrochemical deposition but the final surface after deposition corresponds much better with an area suitable for cell growth with osteophytes.

REFERENCES

[1] A. Jemat, M.J. Ghazali, M. Razali, Y. Otsuka, BioMed Research International **2015**, 791725 (2015).

[2] I.L. Yeo, Materials (Basel) **13** (1), 89 (2020).

[3] G. Zegan, R. Cimpoeşu, M. Agop, I. Ştirbu, D.L. Chicet, B. Istrate, A. Alexandru, B. Anton Prisacariu, Optoelectronics and Advanced Materials-Rapid Communications **10** (3-4), 279-284, (2016).

[4] B. Möller, H. Terheyden, Y. Açil, N.M. Purcz, K. Hertrampf, A. Tabakov, E. Behrens, J. Wiltfang, Int. J. Oral. Maxillofac. Surg. **41** (5), 638-45 (2012).

[5] M.S. Baltatu, C.A. Tugui, M.C. Perju, M. Benchea, M.C. Spataru, A.V. Sandu, P. Vizureanu, Rev. Chim. (Bucharest) **70** (4), 1302-1306 (2019).

[6] T. Berecz, K. Májlinger, I.N. Orbulov, P.J. Szabó, Materials Science Forum **812**, 201-206 (2015).

[7] M. Heydari, M.R. Vaezi, A. Behnamghader, A. Pakseresht, M. Sarmast, Advanced Ceramics Progress **3** (4), 21-24 (2017).

[8] M. Chambard, O. Marsan, C. Charvillat, D. Grossin, P. Fort, Surface and Coatings Technology **371**, 68-77 (2019).

[9] X. Meng, T.Y. Kwon, K.H. Kim, Dental Material Journal **27** (5), 666-671 (2008).

[10] H.B. Hu, C. Lin, P.P.Y. Lui, Y. Leng, J. Biomed Mater Res., **65**A, 24-29 (2003).

[11] Y.Y. Zhang, J. Tao, Y.W. Pang, Y. Wang, T. Wang, Transactiouns of Nonferrous Metals Society of China **16**, 633-637 (2006).

[12] A. Carradò, Journal of Coatings Technology and Research **8**, 749 (2011).

[13] S.A. Abdul Azis, J. Kennedy, P.P. Murmu, F. Fang, P. Cao, Asian Journal of Applied Sciences **7** (8), 745-752 (2014).

[14] C. Domínguez-Trujillo, E. Peón, E. Chicardi, H. Pérez, J.A. Rodríguez-Ortiz, J.J. Pavón, J. García-Couce, J.C. Galván, F. García-Moreno, Y. Torres, Surface and Coatings Technology **333**, 158-162 (2018).

[15] T.T. Li, L. Ling, M.C. Lin, Q. Jiang, Q. Lin, J.H. Lin, C.W. Lou, Nanomaterials (Basel) **9** (5), 679 (2019).

[16] M.S. Safavi, F.C. Walsh, M.A. Surmeneva, R.A. Surmenev, J. Khalil-Allafi, Coatings **11** (1), 1-62 (2021).

[17] H. Farnoush, G. Aldıç, H. Çimenoğlu, Surf. Coat. Technol. **265**, 7-15 (2015).

[18] S. Turk, I. Altinsoy, G. CelebiEfe, M. Ipek, M. Ozacar, C. Bindal, Surf. Coat. Technol. **351**, 1-10 (2018).

[19] M.F.C. Coelho, L.L. de Sousa, C.C. Ferreira, B.F.G. de Souza, E.C. da Silva Rigo, N.A. Mariano, Materials Research Express **6** (12) (2020).

[20] D. Mareci, G. Ungureanu, N. Aelenei, I.M. Popa, I. Cretescu, Studia Universitatis Babes-Bolyai, Chemia, Special Issue, 81-92 (2009).

[21] S. Sobieszczyk, Advances in Materials Science **10** (1), 19-28 (2010).

[22] B.F. Habibovic, C.A. Blitterswijc, K. De Groot, P. Layrolle, J. Amer.Ceram. J. **85**, 517-522 (2002).

[23] Q. Zhang, Z. Leng, Biomaterials **26**, 3853-3859 (2005).

[24] Z. Zou, K. Lin, X. Liu, L. Chen, J. Chang, J. Mater. Chem. **22**, 22637 (2012).

[25] M. Mujahida, S. Sarfraz, S. Amin, Materials Research **18** (3), 468-472 (2015).

[26] A. Afshar, M. Ghorbani, N. Ehsani, M.R. Saeri, C.C. Sorell, Mater. Design **24**, 197 (2003).